Peptide Nanofiber Complexes with siRNA for Deep Brain Gene Silencing by Stereotactic Neurosurgery

Mariarosa Mazza, Marilena Hadjidemetriou, Irene de Lázaro, Cyrill Bussy, and Kostas Kostarelos*

Nanomedicine Lab, Institute of Inflammation and Repair, Faculty of Medical & Human Sciences, AV Hill Building, The University of Manchester, Manchester M13 9PT United Kingdom

ABSTRACT Peptide nanofibers (PNFs) are one-dimensional assemblies of amphiphilic peptides in a cylindrical geometry. We postulated that peptide nanofibers (PNFs) can provide the tools for genetic intervention and be used for delivery of siRNA, as they can be engineered with positively charged amino acids that can electrostatically bind siRNA. The aim of this work was to investigate the use of PNFs as vectors for siRNA delivery providing effective gene knockdown. We designed a surfactant-like peptide (palmitoyl-GGGAAAKRK) able to self-assemble into PNFs and demonstrated that complexes of PNF:siRNA are uptaken intracellularly and increase the residence time of siRNA in the brain after intracranial administration. The biological activity of the complexes was investigated *in vitro* by analyzing the down-regulation of the expression of a targeted protein (BCL2), as well as induction of apoptosis, as well as *in vivo* by analyzing the relative gene expression upon stereotactic administration into a deep rat brain structure (the subthalamic nucleus). Gene expression levels of *BCL2* mRNA showed that PNF:siBCL2 constructs were able to silence the target *BCL2* in specific loci of the brain. Silencing of the *BCL2* gene resulted in ablation of neuronal cell populations, indicating that genetic interventions by PNF:siRNA complexes may lead to novel treatment strategies of CNS pathologies.

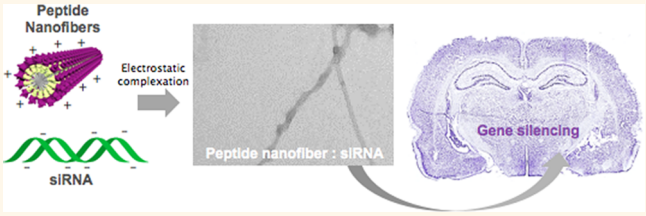

KEYWORDS: gene therapy · brain · neurodegeneration · nanomedicine · CNS

Traditional therapeutics for the treatment of central nervous system (CNS) disorders in the majority of cases are not selective, since small molecular weight agents that can cross the blood–brain barrier (BBB) will distribute into the whole brain parenchyma.[1] A targeted treatment approach to specific neuronal populations in different brain structures may lead to enhanced therapeutic efficacy. RNA interference (RNAi) for post-transcriptional silencing of gene expression could be an approach to target specific genes that need to be switched off in specific neuronal populations involved in the pathogenesis and the symptomatic manifestation of brain morbidities. In an effort to design new tools for genetic intervention in the central nervous system, it is imperative to engineer novel delivery platforms that could achieve efficient intracellular delivery of siRNA and effective silencing *in vivo*. RNAi therapy against CNS diseases should be highly selective and target specific genes in defined brain structures, which is difficult to achieve with current technologies.[2,3] For these purposes, we designed peptide nanofibers (PNFs) to act as molecular transporters of bioactive siRNA that can be used for genetic interventions *via* stereotactic administration in precise brain loci.

Small interfering RNAs (siRNA) are double-stranded, moderately negatively charged, and typically cannot cross plasma membranes. Therefore, gene knockdown can only be achieved by efficient transport of siRNA to the cell cytoplasm. Different materials have been designed as nonviral vectors to overcome the challenge of intracellular delivery of siRNA.[4] Many of the current siRNA delivery technologies employ lipid, polymer, carbon, and inorganic nanoparticles.[5–7] They can electrostatically interact and condense siRNA molecules to (a) protect the siRNA from enzymatic degradation; (b) facilitate cellular internalization; (c) target specific intracellular compartments.[7–9]

PNFs are assemblies of short amphiphilic peptides designed with a hydrophobic tail,

* Address correspondence to kostas.kostarelos@manchester.ac.uk.

Received for review August 11, 2014 and accepted January 9, 2015.

Published online January 09, 2015
10.1021/nn5044838

a β-sheet forming amino acid sequence, and a hydrophilic part, made of basic amino acids, that are positively charged under physiological conditions.[10] This class of peptide amphiphiles was first reported to self-assemble into fibrillar nanostructures by Stupp and co-workers.[11] In little more than a decade, PNFs have found applications in various aspects of regenerative medicine and tissue repair.[12,13] The use of PNF-based hydrogels for neuronal intervention has been explored in several applications. The bioactive IKVAV nanofiber gel[14] has been used as a scaffold for regeneration of descending motor fibers and ascending sensory fibers in a model of spinal cord injury[15] and to induce neuronal differentiation from neuronal progenitor cells.[16] PNFs based on the RADA sequence have been shown to promote axon regeneration and functional return of vision[17] and to reduce acute brain injury and promote functional motor recovery after intracerebral hemorrhage.[18] Also, the transplantation of mouse embryonic stem cells has been facilitated with the use of PNF hydrogels for the treatment of lesions of the auditory nerve.[19]

Aqueous dispersions of PNFs have also been reported to be able to transport bioactive peptides into the CNS[20] and to accumulate in tumors[21] upon systemic administration. Recently we have shown that populations of individualized PNFs can be degraded by blood-circulating enzymes and are cleared from the brain parenchyma within 2 weeks following stereotactic administration in nude mice.[22] PNF-based hydrogel scaffolds have been reported to be able to deliver siRNA *in vitro,*[23] but their efficacy *in vivo* has not been reported. In the present study, we aimed to demonstrate that PNFs can transport siRNA to silence genes in specific brain structures. We investigated the use of PNFs for the transport of siRNA in a spatially localized and therapeutically relevant brain region of the deep brain: the subthalamic nucleus (STN). The gene target used was *BCL2*, able to inhibit apoptosis,[24] hypothesizing that knocking down BCL2 mRNA in the STN will induce apoptosis of the STN neuronal population. PNF:siBCL2 complexes were therefore explored as nanovectors to target localized brain areas by means of stereotactic surgery.

RESULTS AND DISCUSSION

Complexation and Characterization of PNF:siRNA Vectors. Palmitoyl-GGGAAAKRK is a surfactant-like peptide composed of nine amino acids and a palmitoyl chain covalently attached at the N-terminus forming the hydrophobic core of the molecule, as depicted in Figure 1A. It presents three positively charged amino acids that offer an overall positively charged headgroup at physiological pH. Its central core consists of six β-sheet forming amino acids and a hydrophobic palmitoyl chain on opposite ends. The high content of basic residues, also forming the hydrophilic segment of the molecule, is thought to be a common structural feature among other ubiquitous (Tat, penetratin) cell-internalizing peptides.[25] The presence of repeated alanine and glycine residues offer a site for the formation of β-sheet interaction contributing to the self-assembly of single molecules into nanofibers.

An aqueous dispersion of individualized PNFs in 5% dextrose was obtained by probe sonication as previously described.[20,22] The presence of basic residues also offered the possibility to covalently link the *N*-hydroxysuccinimide (NHS) dye VivoTag 680 XL with absorbance close to the near-infrared region that allowed optical imaging *in vivo*. PNFs represent a high-axial-ratio structure, potentially allowing the transport of more than one siRNA molecule per single fiber. We hypothesized that individualized PNFs, not intertwined in aggregates nor entangled in a scaffold matrix, can afford cellular uptake by direct translocation across the plasma membrane similar to previously described mechanisms for other cylindrical, fiber-shaped nanoparticles and nanoneedles.[26−28]

Engineering the PNF surface with basic amino acids could improve their water dispersibility and also allow their positive charges to interact electrostatically with the negatively charged siRNA molecules. An overall cationic surface charge of the complexes would also favor attractive interaction with the plasma membrane, therefore enabling them to act as molecular transporters for intracellular delivery. The presence of Lys-Arg-Lys (KRK) sequences indeed allowed complexation of siRNA onto the PNFs, as evidenced by agarose gel electrophoresis at increasing N/P charge ratios (N = amino group on the PNFs; P = phosphate group on siRNA). The complexes started forming at the 2.5:1 (PNF:siRNA) ratio, while at higher ratios siRNA was not able to migrate in the gel, indicating that complexation with the nanofibers occurred (Figure 1B).

The surface charge (ζ-potential) of the PNF:siRNA complexes at different ratios also confirmed the formation of the complexes. The cationic surface character (positive ζ-potential) of the PNFs became gradually more negative as more amine groups were electrostatically neutralized by the phosphate groups of the nucleic acids to form the complexes (Figure 1B). The morphology of the complexes was further characterized by transmission electron microscopy (TEM). The TEM analysis (Figure 1C−E) revealed the interaction between the PNFs and the siRNA with the appearance of electron-rich, darker objects onto the PNF surface, as the siRNA condensed around the nanofibers. The complexation between PNFs and siRNA (Figure 1C−E) resulted in the formation of fiber-shaped nanoscale vector constructs.

Cellular Internalization of PNF:siRNA Complexes. Small interfering RNAs are negatively charged and very deficient in translocating through the plasma membrane. For this reason, siRNA constructs are commonly

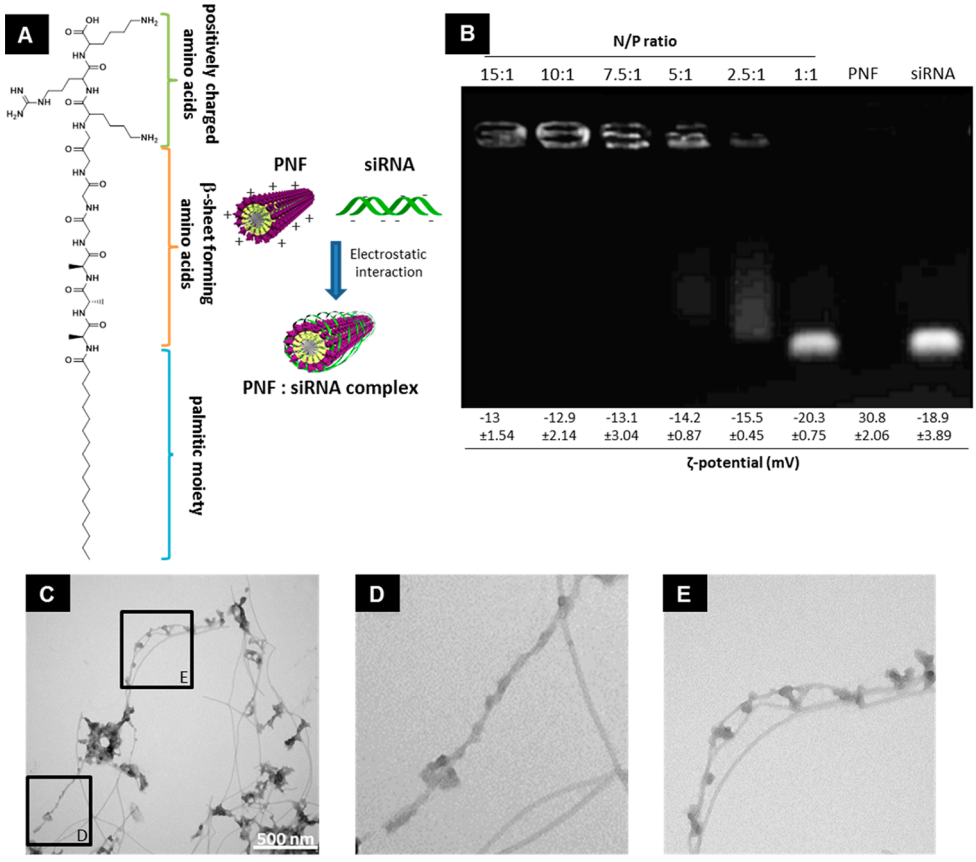

Figure 1. Peptide nanofiber:siRNA complex characterization. (A) Chemical structure of the peptide amphiphile palmitoyl-GGGAAAKRK and schematic representation of the PNFs:siRNA complex formation. (B) Electrophoretic mobility of siRNA complexed with PNFs and surface charge (ζ-potential; mV) values of the complexes. Complexes were formed using 0.5 μg of siRNA at different N/P ratios, and siRNA was visualized by EtBr staining (N = amino group on the PNFs; P = phosphate group on siRNA). (C−E) TEM images of PNF:siRNA complexes formed at 2.5:1 N/P ratio in different magnifications.

conjugated to a ligand or encapsulated in nanoparticles that can facilitate cellular uptake, most commonly *via* endocytotic processes.[29] Endosomal escape is then critically important in order for the siRNA to interfere with the endogenous (cytoplasmic) RNAi pathways in cells. The fiber-like shape of PNFs was thought to offer the possibility of an alternative strategy to achieve endosomal escape or to entirely bypass the endocytic pathway of internalization by direct translocation across the plasma membrane, as described for other high-axial-ratio nanostructures.[26,30]

To interrogate the internalization of these peptide nanofibers within brain cells, we first used primary neuronal cultures. The primary neuron-enriched cell cultures were prepared from hippocampi extracted from E16 fetal rat brains and obtained after a 10 day long incubation in B27 complemented, serum-free medium. Primary neurons were exposed to the PNF suspension when the network of neuronal processes was well-developed (at least 15 days after isolation). Fluorescently labeled PNFs in a 5% dextrose suspension were used in these studies. PNFs were labeled using a dye (VivoTag 680XL) with absorbance close to the near-infrared (NIR) region and incubated with the cells for 4 h. After incubation, the fluorescent signal colocalized within the cell cytoplasm (Figure S1, Supporting Information), suggesting that PNFs were able to translocate within the neuronal cells (Figure S1A, Supporting Information). This agreed with our previously reported observations using other cylindrically shaped nanomaterials (carbon nanotubes) interacting with primary neuron cultures.[31]

To determine the uptake of PNFs and the cellular internalization of siRNA, a noncoding siRNA sequence was fluorescently labeled (siNEG-A546) and complexed with the VivoTag 680XL fluorescently labeled nanofibers. The PNF-VivoTag-680XL: siNEG-A546 complexes were then incubated with two neuronal cell cultures: either rat primary neurons (Figure S1B, Supporting Information) or SH-SY5Y neuroblastoma cells (Figure 2A,B) for 4 h. Confocal microscopy showed that both cell types were able to internalize the PNF:siRNA complexes. Indeed, the fluorescent signals were colocalized as shown in Figure 2B and Figure S1C (Supporting Information), in the red channel for the VivoTag 680 XL on the PNFs and in the green channel for the siNEG-A546 (*i.e.*, a yellow signal demonstrates colocalization). SH-SY5Y cells were also treated with

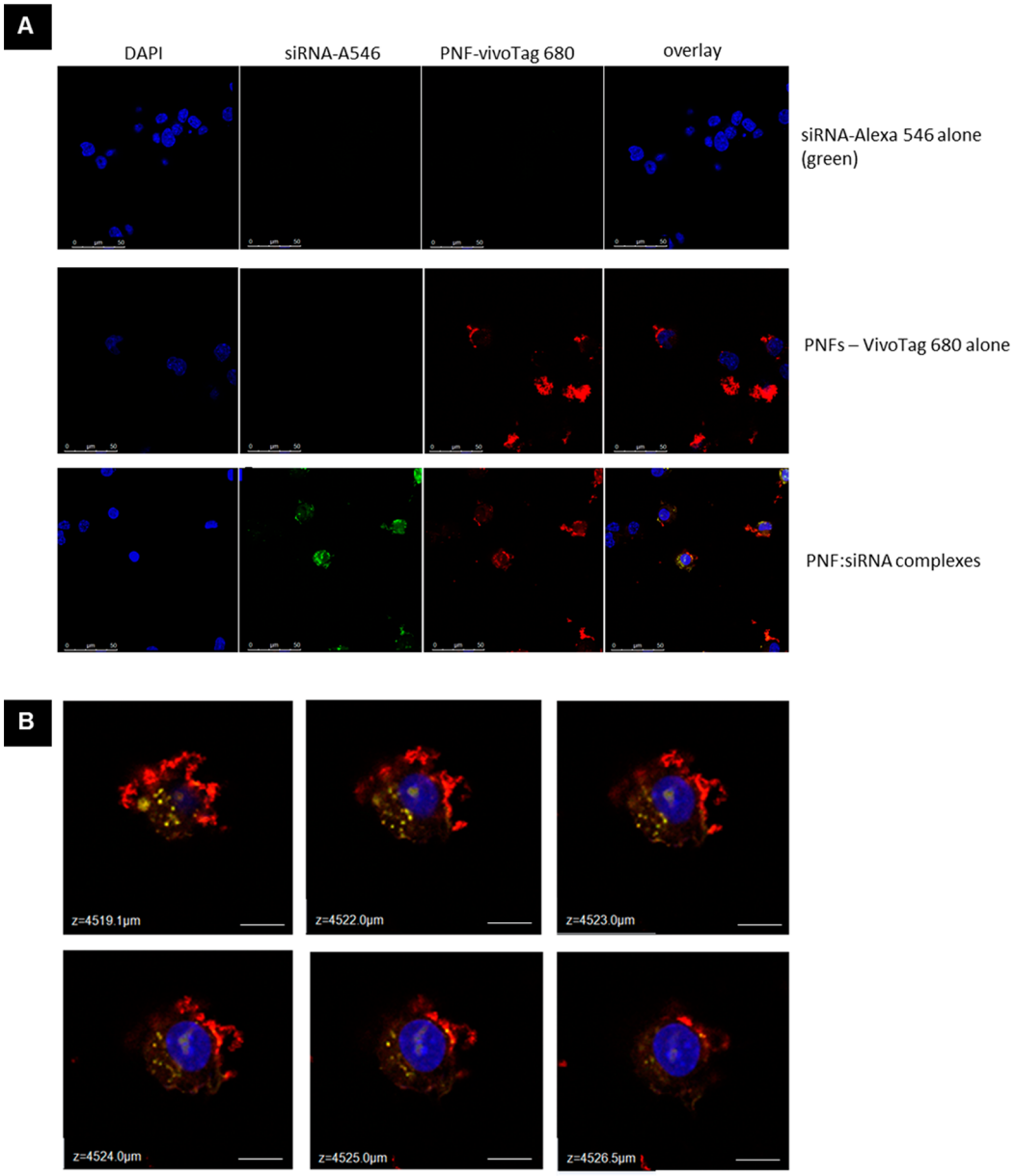

Figure 2. Cellular internalization of PNF:siRNA complexes. (A) Complexes of PNF:siRNA were used to treat human SH-SY5Y cells. PNFs were covalently tagged with Vivo-Tag 680 XL (red), and siRNA was labeled with Alexa 546 (green). Cell nuclei were stained with DAPI (blue); (B) Z-stack of human SH-SY5Y cell incubated with fluorescently labeled PNF:siRNA complexes. Co-localization of red (PNFs) and green (siRNA-A546) signals indicates cytoplasmic localization of the vectors. Scale bar = 10 μm.

naked siNEG-A546 and fluorescently labeled PNFs alone (Figure 2A). Internalization of naked siNEG-A546 did not occur as siRNA is a moderately negatively charged molecule. In contrast, internalization of labeled PNFs alone was evidenced by an intense fluorescent signal recorded in the red channel within the cytoplasm. The fluorescence in the green channel was visible only when cells were treated with PNF:siRNA complexes; thus, cytoplasmic localization of siRNA only occurred by PNF-mediated translocation through the plasma membrane.

A combination of different cellular uptake mechanisms is thought to be involved in the cellular internalization of PNFs. Some types have been previously reported to translocate in the cytoplasm by endocytosis.[32,33] Other alternative systems though, such as the iron oxide dendron-functionalized fiber-shaped nanoparticles[34] carring siRNA (also referred to as dendriworms), have been reported to internalize into cells and reduce protein expression up to 2.5-fold more efficiently than cationic lipids of spherical shape. In the present study, confocal microscopy indicated that PNFs alone could be uptaken by cells and were able to act as vehicles for the intracellular transport of siRNA that otherwise would not be feasible. Much more systematic work is however warranted to elucidate the cell biology mechanisms at play in the internalization of these PNFs.

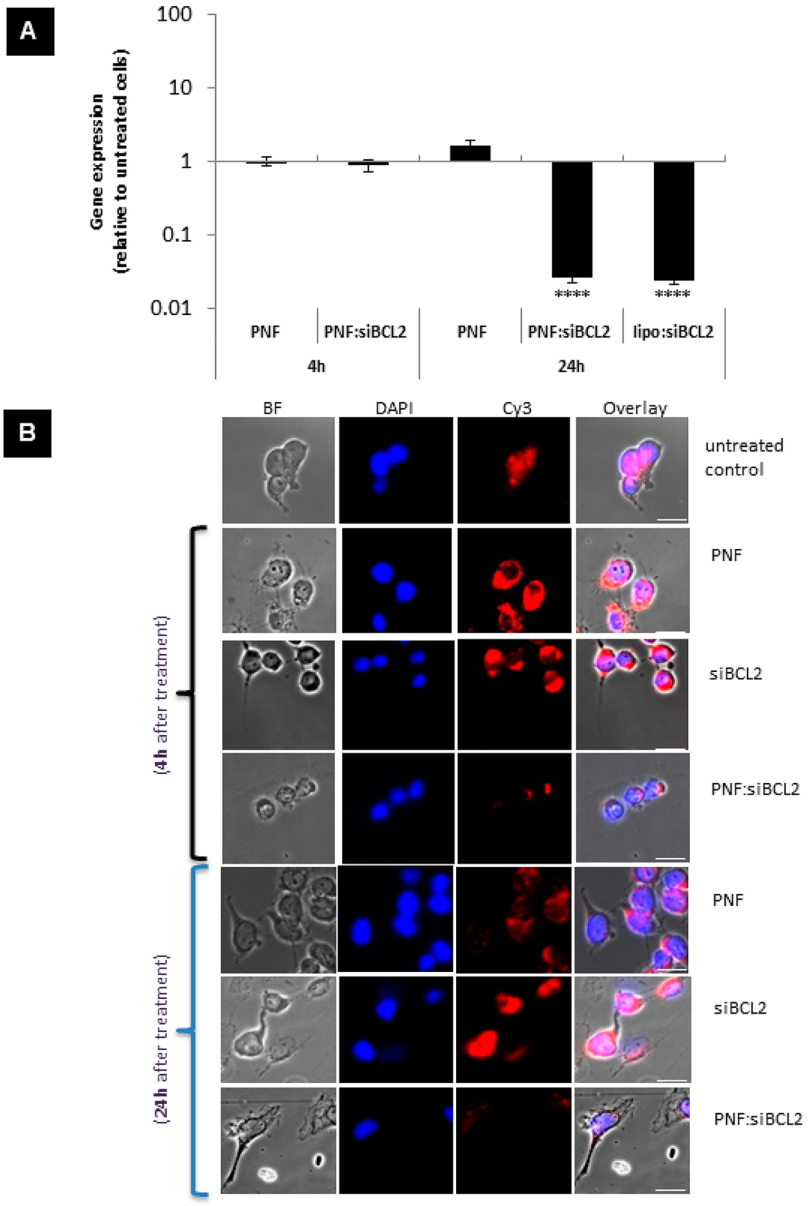

Figure 3. Gene silencing in human neuronal cells (SH-SY5Y) mediated by PNF:siRNA complexes by immunofluorescence. (A) Gene silencing *in vitro* mediated by PNF:siBCL2 measured by quantitative RT-PCR. mRNA BCL2 levels normalized to GADPH after gene silencing using PNF:siBCL2 complexes in SH-SY5Y cell line relative to untreated cells 4 and 24 h post-transfection in comparison to control-treated cells. Data points are average of $n = 3$, and error bars represent s.d. (one-way ANOVA, $p < 0.0001$ against untreated). (B) BCL2 levels after gene silencing using PNF:siBCL2 complexes in SH-SY5Y cell line, in comparison with PNF, siBCL2, control treatment groups. Expression of BCL2 in treated cells was assessed using a primary antibody toward BCL2 and a Cy3-conjugated secondary antibody (scale bar = 20 μm; BF = bright field).

***BCL2* Silencing *in Vitro* and Induction of Apoptosis.** The aim next was to determine the biological activity of the PNF:siRNA complexes *in vitro*. PNF-based hydrogels had been previously reported by Bulut *et al.*[23] to release oligodeoxynucleotides (ODNs) within cells, reporting single-stranded *BCL2* release over 6 days from a peptide nanofiber gel. To test the alternative hypothesis that a free dispersion of individual PNFs (not forming a gel) can act as an effective vector of siRNA and induce gene silencing, we decided to target the *BCL2* gene to knockdown BCL2 protein levels that can lead to induction of apoptosis.[35,36] The ability of the PNFs to act as a transport system for siRNA was first assessed by quantitative RT-PCR. SH-SY5Y cells were transfected with the PNF:siBCL2 complexes for 4 and 24 h, and levels of relative gene expression showed that there is an onset of downregulation at 4 h and statistically significant down-regulation of *BCL2* at 24 h *in vitro* (Figure 3A).

The ability of the PNF:siBCL2 vector to exert its biological activity was assessed *in vitro* by looking at the expression of the BCL2 protein using immunofluorescence. SH-SY5Y cells were transfected with the PNF:siBCL2 complexes for 4 and 24 h, and then cells were

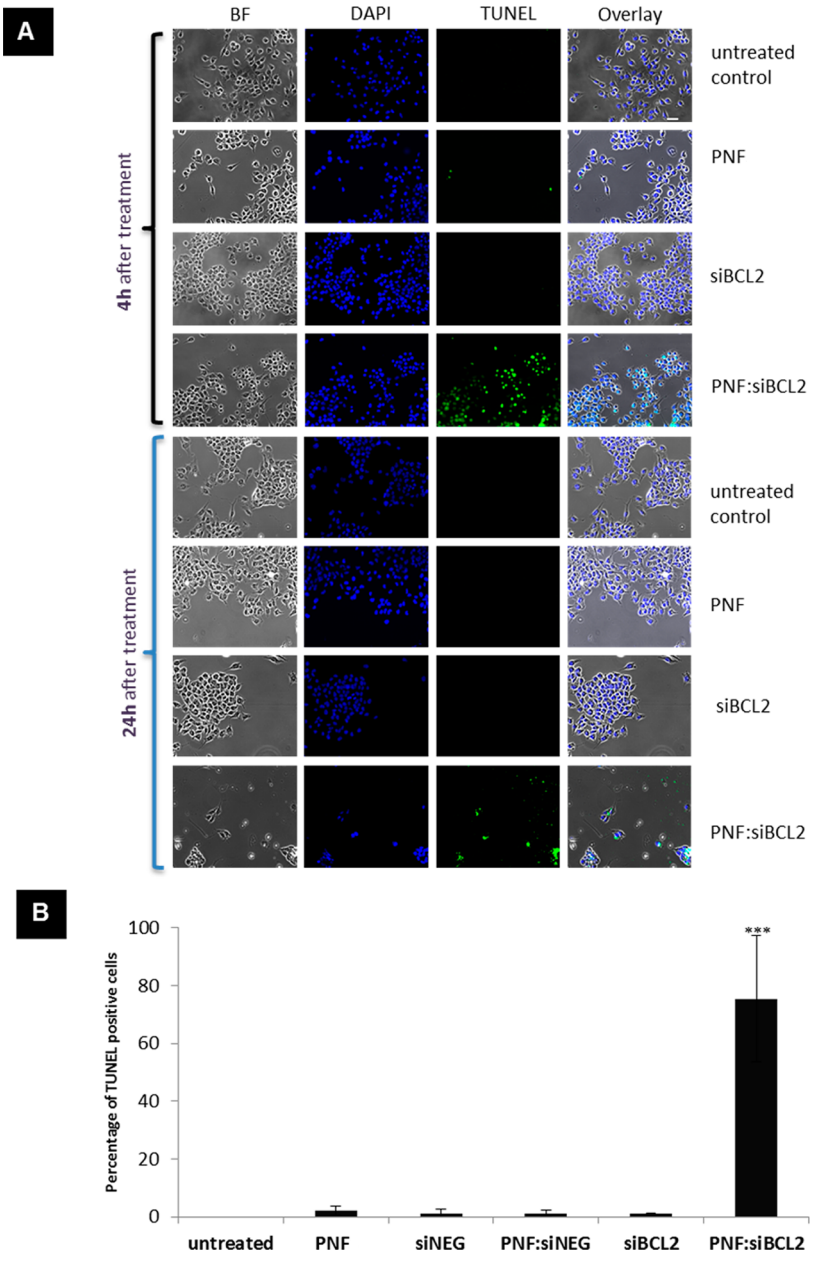

Figure 4. Apoptosis in human neuronal cells (SH-SY5Y) after PNF:siBCL2 vector treatment by TUNEL staining. (A) Apoptotic nuclei are stained in green (TUNEL), and all nuclei are stained in blue (DAPI). After 4 and 24 h post-treatment with PNF:siBCL2, complexes showed large numbers of apoptotic nuclei, and after 24 h of treatment apoptotic bodies were detected only in the PNF:siBCL2 treatment group. Scale bar is 40 μm (BF = bright field). (B) Quantitation of TUNEL positive cells. TUNEL positive cells were measured through the ratio between TUNEL positive nuclei relatively to DAPI stained nuclei and expressed in percentage. Nuclei were counted using ImageJ. Statistical analysis was performed using one-way ANOVA ($p < 0.0001$ against untreated).

fixed and stained to reveal the levels of BCL2 expression. Figure 3B shows that cells treated with the PNF:si-BCL2 complexes were exhibiting decreased levels of BCL2 protein expression as early as 4 h post-treatment compared to naive (untreated) cells and various control-treated cells (naked siBCL2, siNEG, PNF:siNEG and PNFs alone; Figure 3B and Figure S2C, Supporting Information). The specificity of the BCL2 antibody was assessed by treating the transfected cells with the secondary antibody alone (tagged with Cy3) (Figure S2A, Supporting Information) with no detectable signal obtained. Immunofluorescence of the transfected cells also revealed activation of Caspase-3 as early as 4 h post-transfection (Figure S2B, Supporting Information). Reduction in the levels of BCL2 protein expression is associated with the conversion of inactive pro-caspase to caspase-3 directly involved in the cascade that ultimately drives cells to apoptosis.[37]

Cell apoptosis was further confirmed with the TUNEL assay that marks DNA fragmentation and apoptotic bodies[38](Figure 4A,B and Figure S3, Supporting Information). At 4 hours post-transfection with the PNF:siBCL2 vectors, the majority of cells were shown

to be TUNEL positive. The induction of apoptosis was sequence-specific since scrambled siRNA (siNEG) delivered as a complex with PNFs did not trigger apoptosis. Twenty-four hours post-treatment with the PNF:siBCL2 complexes, the remaining cells were displaying characteristic features of chromatin condensation and apoptotic bodies. The presence of residual bodies demonstrated that these cells were in the final stages of apoptosis.

The cytotoxicity of PNFs alone was also assessed by measuring the release of the cytoplasmic enzyme lactate dehydrogenase (LDH) at increasing doses. First SH-SY5Y cells were incubated in serum-free media with PNFs, and after 4 h, cells were recovered by adding FBS-supplemented media to mimic the experimental conditions used in the transfection protocol. In serum-free media conditions (4 h after treatment), the positive charge on the PNFs surface proved to affect the integrity of the cells membrane. LDH enzyme levels in the supernatant were comparable to that of 1% Triton for concentrations above 0.5 μg/mL (Figure S2A, Supporting Information). After 4 h, cells were allowed to recover for another 20 h by addition of FBS to the media to a total 10%. Cells exposed to concentrations up to 10 μg/mL were able to recover over 24 h. Only the cells exposed to the highest concentrations (50−100 μg/mL) showed enzyme release comparable to that of the positive control. Cells that were exposed to PNFs in serum-supplemented media were less susceptible to cytotoxicity both at 4 and 24 h, and the total amount of LDH released was statistically lower in comparison to the positive control for all the doses both at 4 and 24 h. These data suggested that the interaction between serum proteins and the positively charged PNFs will influence the interaction and safety profile of these materials with cells.

Peptide conjugates with siRNA have been previously investigated as *in vivo* delivery agents.[5] However, the negatively charged backbone of siRNA conjugated only to a short peptide sequence can neutralize basic residues or sterically hinder the peptide site from interaction with the plasma membrane and receptors, thus decreasing the overall translocation efficiency of the peptide. PNFs offer a high axial surface area for siRNA complexation, allowing excess cationic surface functions to be available for interaction with the plasma membrane and therefore improved cellular uptake (Figure 1C−E). Peptides can also constitute components of alternative vector systems that form nanoparticles with siRNA as their payload. Different sequences, possessing cationic and hydrophobic residues, have been identified and grouped under the umbrella of "cell penetrating peptides" and extensively exploited to engineer nanoparticles with enhanced cell internalization capabilities.[39] However, efficient cellular uptake does not always translate to effective gene silencing, since subsequent endosomal escape of the nucleic acid will dictate the efficacy of the RNAi process, as documented for peptide-engineered liposomes.[40] Quantification of cytosolic siRNA release in liver, after intravenous administration of lipid nanoparticles used as nucleic acid carriers, showed that only 1−2% of the total siRNA taken up by hepatocytes was released in the cytosol after 6 h.[29]

When PNF-based vectors were compared to conventional transfection agents (Lipofectamine 2000), more cells were found to undergo apoptosis after 4h of treatment with PNF:siBcl2, as shown in Figure S4A (Supporting Information). One possible explanation is that the siRNA can be transported more efficiently into the cytosol due to PNF-mediated trespassing of endosomal internalization, *via* direct translocation through the plasma membrane. Confocal microscopy indicated (Figure 2B and Figure S1C, Supporting Information) that the colocalized signal of the PNF:siRNA complexes was found throughout the cytoplasm (and not restricted to endosomal compartments). Moreover, the ability of PNF:siRNA complexes to translocate directly into the cytosol translated into an earlier apoptosis induction for most of the cells at 4h after transfection, in comparison to lipofectamine-mediated siRNA delivery (Figure 4 and Figure S4, Supporting Information). Peptide-mediated siRNA complexes have been previously reported to be effective carriers of siRNA delivery but usually show silencing effects only 12−48 h after transfection.[41−44] PNFs seem to provide a faster and more efficient delivery of siRNA into the cytoplasm compared to other peptide-based siRNA delivery vectors. Further work is warranted to elucidate such cellular internalization mechanisms.

PNF:siRNA Complexes in the Brain: Residence Time and Gene Silencing *in Vivo*. *BCL2* is a key gene in suppressing cell death in the central nervous system (CNS).[45,46] Triggering apoptosis may be exploited for therapeutic purposes in those pathologies where specific cell populations may need to be ablated. For instance, ablation of neuron populations of the subthalamic nucleus (STN) by means of *BCL2* gene expression silencing may have clinical relevance in the treatment of neurological disorders that are caused by the overactivation of glutamatergic neurons in the STN, as in the case of Parkinson's Disease (PD).[47−49] Ablation of STN neurons by a single stereotactic injection of PNF:siBCL2 complexes could offer a complementary tool for surgical ablation of STN neurons, in concert or synergy with clinically established neurosurgical procedures, such as deep brain stimulation (DBS).[48,50]

In the present study, our aim was to investigate whether apoptosis of neuronal tissue in the subthalamic nucleus (STN) could be induced by means of stereotactically administered PNF:siBCL2 vectors. The complexes were administered in the right-hand-side STN of the rat brain (coordinates were 2.5 mm lateral, 3.8 mm posterior to bregma and 7.6 mm ventral to the

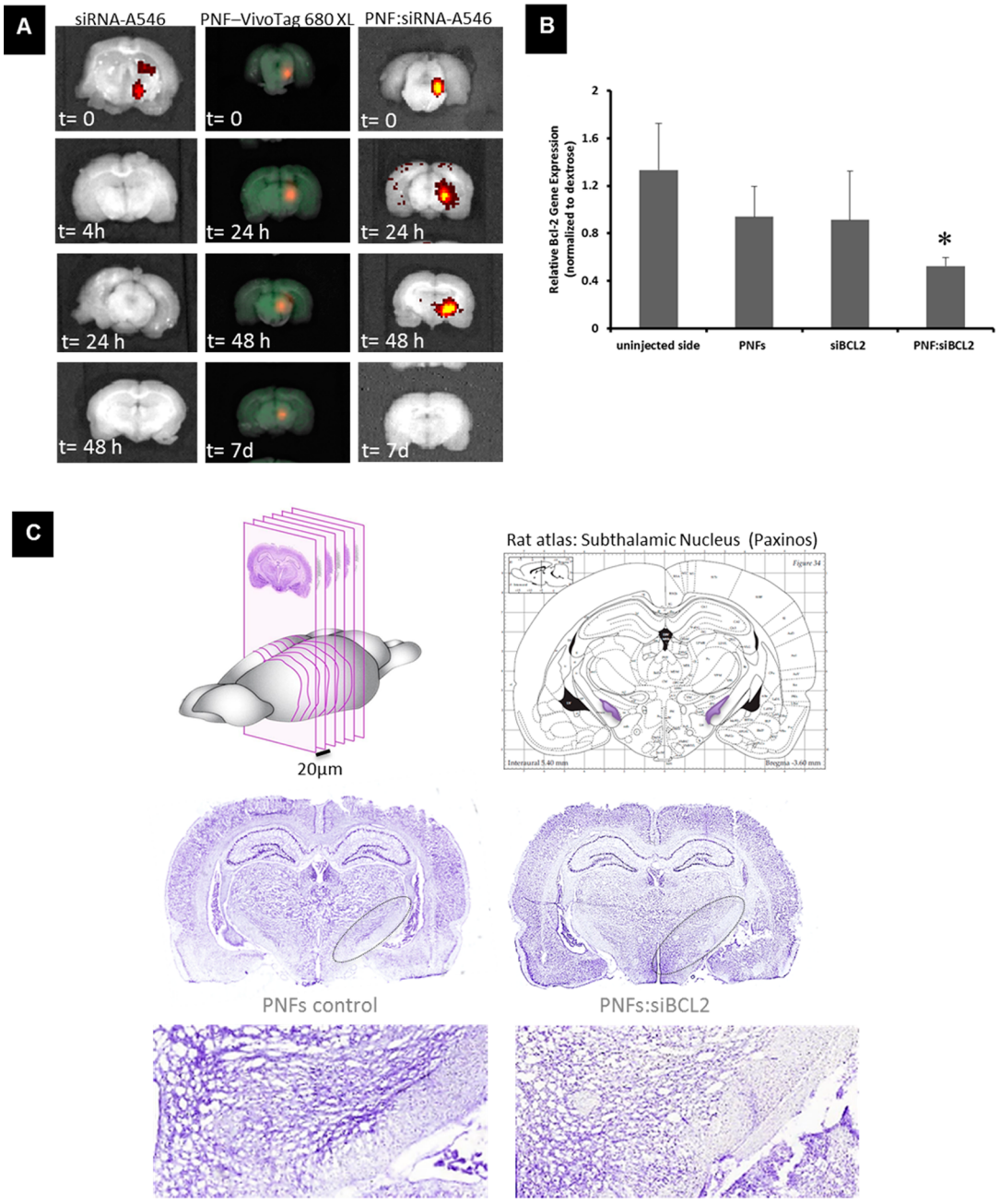

Figure 5. *In vivo* **administration of PNF:siRNA complexes and gene silencing. (A) Residence time of PNF:siRNA in the brain and BCL2** *in vivo* **silencing.** *Ex vivo* **rat brain coronal sections of siRNA-A546 (left panel; control siRNA), fluorescently labeled PNFs only (central panel; labeled with VivoTag 680 XL), and PNF:siRNA-A546 complexes (right panel), injected in the subthalamic nucleus (STN) at different time points. (B) BCL2 gene silencing** *in vivo* **achieved upon localized injection of PNF:siBCL2 complexes in the STN of the right brain hemisphere (*, $p \leq 0.1$) by RT-qPCR. (C) Light microscopy of Nissl-stained coronal sections at the level of the STN. Loss of STN neurons (circled areas) can be observed only in the PNF:siBCL2 treated brain (right side). The circled areas are magnified in the bottom panels respectively for PNFs control and PNF:siBCL2.**

dura).[51] A key aspect for a successful neurosurgically precise technology is confirmation that the vectors can remain at the site of injection with no spread to distal brain structures. To address this question, the residence time of VivoTag 680 XL-labeled PNFs was monitored over a period of 7 days postinjection by using an IVIS Lumina II imaging system. The residence time of Alexa-Fluor 546-labeled siRNA complexed to PNFs was also separately recorded in order to cross-register the siRNA localization and stability against *in vivo* enzymatic degradation over time. As shown in Figure 5A, complexation with the nanofibers resulted in retention of fluorescently labeled siRNA at the site of injection up to 48 h (Figure 5A, right panel), while PNFs were detected in the brain up to 7 days (Figure 5A, central panel). In both experiments, the fluorescent signal from the PNFs alone (central panel) and the complexes with siRNA (right panel) remained localized in the right

brain hemisphere, in close proximity to the injection area. Naked siRNA-Alexa546 at the same concentration was injected in the same stereotaxic coordinates (left panel) to indicate that the naked nucleic acid signal disappeared from the area of injection shortly after administration. A rather diffuse fluorescent signal was detected immediately after surgery (t = 0), but no signal was detected at later time points (4−48 h) presumably due to the reported biological instability of the molecule. These results suggested that the PNF:siRNA complexes did not diffuse or migrate in distal structures of the brain, and remained in close vicinity to the injection site even 1 week after the stereotactic administration.

Next, the ability of PNFs to deliver biologically functional siRNA was assessed by studying the *in vivo* gene silencing activity after stereotactic injection in the right STN of normal rat brains. Twenty-four hours postinjection and surgery, the STN was dissected from the harvested brains and mRNA expression levels assessed using quantitative RT-PCR. Figure 5B shows that the PNF:siBCL2 complex successfully silenced the expression of BCL2 in the STN in comparison to the noninjected hemisphere and other groups of control-treated animals, albeit with limited power of statistical significance, due to the scale of the experimental design (n = 3−4). Cellular ablation resulting from *BCL2* gene silencing in the STN was then assessed by evaluation of structural changes in the STN region by using Nissl staining. Figure 5C shows that administration of the PNF:siBCL2 vectors in the right STN resulted in significant loss of the Nissl-stained cells in this brain structure (highlighted by the circled areas) in comparison to the left hemisphere (noninjected side). Our results suggested ablation of neuronal tissue only in the STN of animals administered with the PNF:siBCL2 vectors in comparison to those that were treated with the PNFs alone.

RNAi therapy has shown potential as a treatment option in neurodegenerative disorders.[2] In the case of PD, localized siRNA-mediated knockdown has been explored as a strategy for the suppression of α-synuclein in the substantia nigra of the nonhuman primate brain. Interestingly, direct infusion of siRNA showed a remarkable decrease of 40−50% in protein expression in the treated hemisphere in comparison to the noninjected hemisphere.[52] However, direct infusion of free siRNA for neuronal ablation may not be a suitable approach, as it may reach distal structures and interfere with other brain regions and therefore result in off-target effects. An alternative, much more developed strategy to localized gene therapy is the stereotactic injection of viral vectors.[53] However, despite promising data based on preclinical evaluation of these vectors, concerns related to both efficacy and safety have emerged after the publication of the results of one of the most advanced adeno-associated virus (AAV)-based trail called CERE-120. The phase II clinical trial results showed that efficacy in treated patients was not improved in comparison to patients who have undergone sham surgery, and that one-third of the patients developed adverse effects as a consequence of the treatment.[54]

A novel nonviral vector platform for localized siRNA delivery is described in the present study that can result in lower levels of *BCL2* gene expression in brain structures leading to downstream ablation of neuronal tissue. Such observations are considered encouraging, however a lot more work will need to be undertaken to assess the safety and therapeutic efficacy imparted by the neurosurgically localized gene knockdown activity obtained from PNF:siRNA vectors in different therapeutic models.

CONCLUSION

This study offered proof-of-principle evidence that populations of individualized PNFs can form complexes with biologically active siRNA and facilitate its efficacious intracellular transport. PNFs acted as intracellular transporters of siRNA both *in vitro* and *in vivo*. The siRNA maintained its biological activity following complexation with the nanofibers, leading to decreased gene expression and protein levels. PNF:siRNA complexes that achieve localized gene silencing in specific deep brain structures could potentially be used both as a tool for *in vivo* gene identification or for the development of gene silencing therapeutics of brain diseases.

EXPERIMENTAL SECTION

Preparation of PNFs and PNFs:siRNA Complexes and Assessment of Complexation by Gel Electrophoresis. The palmitoyl-GGGAAAKRK peptide amphiphile was custom-made by Peptide Synthetics (Cambridge, UK) as freeze-dried powder at 95% purity. PNFs were prepared from a dispersion of 1 mg/mL peptide amphiphile in 5% dextrose (pH = 6.4) filtered through 0.22 μm Millipore membrane filter. The dispersions were subjected to 5 min of probe sonication at 20% of the maximum amplitude alternate pulsed sonication of 20 s each. Complexes were prepared by mixing 0.5 μg of siRNA (AllStars Negative Control siRNA, Qiagen; Cat. No. 1027281) at different N/P charge ratios (1:1, 2.5:1, 5:1, 7.5:1, 10:1, 15:1). Complexes were incubated at room temperature for 30 min to allow complete formation. Complexation efficiency was assessed by loading PNF:siRNA complexes onto 1% agarose/TBE gel containing ethidium bromide (0.5 mg/mL). Naked siRNA and PNFs were included for comparison. The gel was run for 45 min at 70 V and visualized under UV light using GeneSnap (G:Box, Syngene, UK).

ζ-Potential. The overall charge of the complexes was estimated by measuring the Z-potential as a function of the electrophoretic mobility on a Malvern Zetasizer unit, Nano ZS series HT at 25 ± 0.1 °C by loading the sample dispersions in a U-shaped cuvette, equipped with gold electrodes.

Transmission Electron Microscopy. TEM was performed using a Phillips Biotwin CM 210 electron microscope. Samples were prepared by transferring 10 μL onto a 300 grid copper mesh, and the drop was allowed to adsorb on top of the mesh for 10 s after which the excess was wicked off using the edge of a filter disk. Uranyl acetate 1% (w/v) was used as a negative contrast agent, which was applied to the mesh, allowed to stand for approximately 5 s, and then removed using the edge of a filter disk. The copper grid was then introduced into the TEM column for imaging.

Preparation of Fluorescently Labeled PNFs. As previously reported,[22] VivoTag 680 XL dye (absorbance at 688 $\pm$ 5 nm; PerkinElmer) was reconstituted with 1 mL of DMSO. A 1 mg/mL suspension was made using the freeze-dried peptide and phosphate-buffered saline. This suspension was transferred into an amber Eppendorf tube to protect it from light. Sodium bicarbonate (50 μL of 1 M solution) and 2 μL of VivoTag 680 XL in DMSO were added. Tubes were maintained under constant agitation into a Tissuelyser (Qiagen) and set to oscillate 15 times/s for 2 h. The suspension was then centrifuged at 12000 rpm for 4 min. The supernatant that contained unreacted dye was removed and discarded. The pellet was resuspended in 500 μL of distilled water which was filter sterilized by a 0.22 μm cellulose acetate syringe filter. The tubes were then centrifuged at 12000 rpm for 4 min, after which the supernatant was removed along with any remaining unreacted dye. The pellet was finally resuspended in filter sterilized dextrose 5% (w/v) to give a final concentration of 1 mg/mL. The prepared samples were then bath sonicated for 5 min using the alternate pulsed sonication of 20 s each. Samples were stored at 4 °C until needed.

Cellular Uptake Studies Using Confocal Microscopy. The human neuroblastoma SH-SY5Y cell line was used for the *in vitro* experiments (Figure 2). Cells were grown in DMEM complemented with 10% FBS (Fetal bovine serum), 1% nonessential amino acids, and 1% of penicillin−streptomycin in a humidified 37 °C/5% CO_2 incubator. Cells were passaged when they reached 80% confluence for a maximum of 20 passages in order to maintain exponential growth.

Neuron-enriched cell cultures were prepared from hippocampus extracted from E16−E18 Wistar fetal rat brains (standard Witschi stages 33−34). Hippocampal tissue pieces were dissociated to single cell suspensions by trypsinization followed by mechanical trituration in Ca_2^+/Mg_2^+ free HBSS solution. After determination of the number of live cells, 50 thousands cells per well were plated onto poly-L-lysine (50 μg/mL) coated glass bottom 8 well chamber slide (Millicell EZ SLIDE, Merck-Millipore) with DMEM:F12 medium completed with 12% heat inactivated fetal bovine serum and incubated at 37 °C in a humidified 5% CO_2 incubator. After 12 h, medium was changed to serum free Neurobasal Medium supplemented with B27, glutamine (0.5 mM), penicillin (100 U), and streptomycin (100 μg). B27 supplement was used as a means to reduce glial cells growth and to obtain a nearly pure neuronal cell culture. Cultures were incubated in a humidified 37 °C/5% CO_2 incubator for 10 days before experimentation. Cell culture reagents (PBS, HBSS, trypsin, fetal bovine serum, DMEM:F12, neurobasal, B27, antibiotics) were purchased from Gibco (Life technologies, UK). Medium was changed by half every 3 days.

AlexaFluor 546-labeled siNEG (siNEG AF546) (5′−3′: UGCGCUACGAUCGACGAUG) (Eurogentec, UK) was complexed to VivoTag 680 XL labeled PNFs at a 2.5:1 N/P ratio (80 nM final siRNA concentration). Images were acquired on a confocal laser scanning LSM 710 microscope (Carl Zeiss) or on a Mp_OPO SP8 (Leica) used in confocal mode. DAPI was used as nuclear staining.

***In Vitro* Real-Time PCR Analysis.** SH-SY5Y cells were seeded in six-well plates and allow to reach 60−80% confluence prior treatment. Cells were transfected in serum-free media using PNF:siBCL2 and controls of PNFs and Lipofectamine:siBcl2 with a final concentration of siBCL2 and siNEG of 80 nM. All experiments were performed in triplicate. Total RNA was extracted with a Macherey-Nagel kit according to the manufacturer's instructions. The concentration of total RNA was determined by measuring the optical density on an Eppendorf Biophotometer Plus, and the purity was checked as the 260 nm/280 nm and 260 nm/230 nm ratios with expected values between 1.8 and 2.0. First-strand cDNA was prepared from 1 μg of RNA in a total volume of 20 μL using the iScript cDNA synthesis kit (Biorad). Real-time PCR was performed using the CFX96 Real-Time PCR detection system (BioRad). The reactions contained 1× Fast SYBR Green Master Mix (BioRad), each primer (see primer table for sequences) at 200 nM and 2 μL of cDNA from reverse transcription PCR in a 25 μL reaction. After an initial denaturation step at 95 °C for 10 min, amplification was carried out with 40 cycles of denaturation at 95 °C for 10 s and annealing and elongation at 60 °C for 30 s. Amplification was followed by a melting curve analysis to confirm PCR product specificity. No signals were detected in no-template controls. All samples were run in triplicate, and the mean value of each triplicate was used for further calculations. Relative gene expressions were calculated using the $\Delta\Delta C_T$ method. The quantity of GAPDH (housekeeping) transcript in each sample was used to normalize the amount of each transcript, and then the normalized value was compared to the normalized expression in naïve samples to calculate a fold change value. The statistical significance of the results $\pm$ SD was evaluated using the One way ANOVA analysis followed by analysis with the Dunnett test with 95% confidence interval.

Immunofluorescence. siBCL2 (5′−3′: AAGTTCGGTGGGGTCATGTGT) was purchased from Qiagen (cat. no. SI00299404). SH-SY5Y cells were seeded onto Millicell EZ slides (Millipore) eight-well glass (8000 cells/well). After 24 h of cell culture expansion, cells were transfected in serum free conditions with PNF:siBCL2 (n = 4) and controls of PNFs (n = 2), siBCL2 (n = 2), siNEG (n = 2), and PNF:siNEG (n = 2), with a final concentration of siBCL2 and siNEG of 80 nM. Two independent repeats were performed for each group. Cells were then incubated for 4 h without serum at 37% in 5% CO_2. After that, cells were fixed by methanol precooled at −20 °C. The cells were then washed two times with PBS, washed with 0.1%Triton in PBS on the shaker for 5 min, blocked with 5% NGS and 0.1% Triton in PBS for 1 h, and washed once with 0.1% Triton−2% BSA in PBS. Cells were then incubated with the BCL2 primary antibody (ab7973, Abcam) or with the Caspase-3 (ab32351, Abcam) diluted in a mixture of 0.1% Triton−2% BSA in PBS (dilution 1:100) for 2 h at rt in a humidified chamber. After that, the cells were washed three times with the mixture of 0.1% Triton−2% BSA in PBS. Then, the cells were incubated with the following secondary antibody: Cy3-conjugated goat antirabbit IgG (1:125 Jackson, Immunoresearch) diluted in 5% NGS and 0.1% Triton in PBS and washed three times with 0.1% Triton in PBS and once with PBS only. Slides were mounted with Vectashield medium containing DAPI (Vector Laboratories) to stain the nuclei. Samples were imaged using a Zeiss Axiovision Fluorescence Microscope. To check the specificity of the assay, cells were also treated only with the secondary antibody. For the 24 h treatment experiment, following 4 h of incubation in serum-free conditions, serum was added to each well to achieve a final concentration of 10%, and cells were then incubated at 37% in 5% CO_2 for a further 20 h before proceeding with the immunofluorescence staining as described above.

TUNEL Assay. To detect apoptosis of cells, a DeadEnd fluorometric TUNEL assay kit (Promega) was used according to the manufacturer instructions. All experiments were performed with a minimum of three independent measurements. Cells were transfected with PNF:siBCL2 and controls of PNFs, siBCL2, siNEG, and PNF:siNEG, Lipofectamine2000:siBCL2 under serum-free conditions with a final concentration of siBCL2 and siNEG of 80 nM. Lipofectamine 2000:siBCL2 complexes were also prepared according to the manufacturer's protocol (Lipofectamine2000, Life Technologies, UK). Native cells, cells treated with siBCL2, and cells treated with siNEG were used as controls. Slides were mounted with Vectashield medium containing DAPI (Vector Laboratories) to stain the nuclei, and coverslips were added. Samples were imaged using a Zeiss Axiovision Fluorescence Microscope. Processing of images obtained from fluorescent microscopy was performed using NIH ImageJ and results expressed as percentage of apoptotic (TUNEL) nuclei relatively to the total number of DAPI stained nuclei. Results are presented as the mean $\pm$ s.d. and were analyzed using one-way ANOVA using the Dunnett test with 95% confidence interval.

LDH Assay. SH-S5Y5 cells were seeded in a 96-well plate at a density of 5000 cells/well and cultured until they reached 60−80% confluence. PNF treatment groups (n = 6) were as follows: 0.05, 0.1, 0.5, 1, 5, 10, 50, and 100 μg/mL. LDH enzyme release was measured using the CytoTox 96 nonradioactive cytotoxicity assay (Promega) following manufacturer instructions. Media were sampled 4 and 24 h after treatment and normalized with 1% Triton X-100-treated positive control representing 100% LDH release.

***In Vivo* Experiments.** All experiments were performed in accordance with the approved recommendations and policies of the UK Home Office (Animal Scientific Procedures Act 1986, UK). Adult male Sprague−Dawley rats were raised in standard conditions caged in groups of four animals with free access to food and water.

IVIS Imaging. Groups of animals (n = 3) were anesthetized by inhalation of isoflurane and intracranially injected with fluorescently labeled siRNA-A546 complexed in the form of PNF:siRNA-A546 at stereotactic coordinates: 2.5 mm lateral, 3.8 mm posterior to bregma, and 7.6 mm ventral to the dura.[51] Immediately after injection (t = 0 h), 24 h, 48 h, or 7 days after injection, brains were harvested, and coronal sections were cut at about 3 mm thickness. Sections were imaged using an IVIS Lumina II epi-fluorescent camera (Perkin Elmer), using excitation wavelength of 465−535 nm and emission filter set at 580−620 nm for the detection of siRNA-A546 and excitation wavelength of 675 nm and emission filter set at 700−840 nm.

Stereotactic Administration Therapy into STN. Unilateral injections into the right subthalamic nucleus (STN) were performed at stereotactic coordinates: 2.5 mm lateral, 3.8 mm posterior to Bregma, and 7.6 mm ventral to the dura.[51] A 1 μL solution containing the complex of 414 ng PNFs and 174.5 ng siBCL2 was injected into the STN of the right hemisphere of rats (n = 4) at a rate of 1 μL over 3 min. For comparison, groups of rats were injected with 1 μL containing the vehicle alone (5% dextrose; n = 3), PNFs (171 ng, n = 4), or uncomplexed siBCL2 (91.2 ng; n = 4) in 5% dextrose in water. After stereotactic injection of the treatment, the syringe was maintained in place for 3 min before being slowly withdrawn. During surgical procedures, animals were oxygenated and heated to ensure a 37 °C rectal temperature. After recovery, the animals were returned to their cages.

Real-Time PCR Analysis of *ex Vivo* Tissues. Total RNA was extracted with a Macherey-Nagel kit according to the manufacturer's instructions. The concentration of total RNA was determined by measuring the optical density on an Eppendorf Biophotometer Plus, and the purity was checked as the 260 nm/280 nm ratio with expected values between 1.8 and 2.0. First-strand cDNA was prepared from 1 μg of RNA in a total volume of 20 μL using the iScript cDNA synthesis kit (Biorad). Real-time PCR was performed using the CFX96 Real-Time PCR Detection System (BioRad). The reactions contained 1× Fast SYBR Green Master Mix (BioRad), each primer (see primer table for sequences) at 200 nM, and 1 μL of cDNA from reverse transcription PCR in a 25 μL reaction. After an initial denaturation step at 95 °C for 10 min, amplification was carried out with 40 cycles of denaturation at 95 °C for 10 s and annealing at 60 °C for 30 s. Amplification was followed by a melting curve analysis to confirm PCR product specificity. No signals were detected in no-template controls. All samples were run in triplicate, and the mean value of each triplicate was used for further calculations. Relative gene expressions were calculated using the $\Delta\Delta C_T$ method. The quantity of GAPDH (housekeeping) transcript in each sample was used to normalize the amount of each transcript, then the normalized value was compared to the normalized expression in naïve samples to calculate a fold change value. The statistical significance of the results ± s.d. was evaluated using the One way ANOVA analysis followed by analysis with the Dunnett test with 90% confidence interval.

Cryosectioning and Nissl Staining. Brains used for Nissl staining were harvested 3 weeks after administration of treatment. Rat brains were cut with a Leica CM3050S cryostat to produce coronal sections of 20 μm. Sections were mounted on positively charged glass slides and allowed to air-dried. Slides were immersed in Histoclear (National Diagnostics) for 30 min and hydrated in absolute ethanol for 10 min, 95% ethanol for 3 min, and 70% ethanol for 3 min before being rinsed in tap water and distilled water. Slides were then stained with warm 0.1% cresyl violet solution (40 °C) for 10 min, rinsed in distilled water, differentiated in 95% ethanol (10 min), dehydrated in 100% ethanol (10 min), and cleared in Histoclear for 10 min. Slides were mounted using permanent mounting medium and imaged using a 3DHISTECH Pannoramic 250 flash slide scanner.

Conflict of Interest: The authors declare no competing financial interest.

Acknowledgment. We thank Miss Katie Bates for help with the stereotactic injections and husbandry of the animals used in the study. This work was partially funded by the University of Manchester, the European Commission Marie Skłodowska-Curie Actions (Intra-European Fellowship, PIEF-GA-2010-276051, NANONEUROHOP)), and the Engineering and Physical Sciences Research Council (Grand Challenges in the Application of Nanotechnology in Healthcare).

Supporting Information Available: Figures S1−S4. This material is available free of charge *via* the Internet at http://pubs.acs.org.

REFERENCES AND NOTES

1. Pardridge, W. M. Drug Transport Across The Blood−Brain Barrier. *J. Cereb. Blood Flow Metab.* **2012**, *32*, 1959–1972.
2. Boudreau, R. L.; Rodriguez-Lebron, E.; Davidson, B. L. RNAi Medicine For The Brain: Progresses And Challenges. *Hum. Mol. Genet.* **2011**, *20*, R21–27.
3. Dessy, A.; Gorman, J. M. The Emerging Therapeutic Role of RNA Interference In Disorders Of The Central Nervous System. *Clin. Pharmacol. Ther.* **2011**, *89*, 450–454.
4. Kanasty, R.; Dorkin, J. R.; Vegas, A.; Anderson, D. Delivery Materials For siRNA Therapeutics. *Nat. Mater.* **2013**, *12*, 967–977.
5. Coursindel, T.; Jarver, P.; Gait, M. J. Peptide-Based In vivo Delivery Agents For Oligonucleotides And siRNA. *Nucleic Acid Ther.* **2012**, *22*, 71–76.
6. Bates, K.; Kostarelos, K. Carbon Nanotubes As Vectors For Gene Therapy: Past Achievements, Present Challenges And Future Goals. *Adv. Drug. Delivery Rev.* **2013**, *65*, 2023–2033.
7. Musacchio, T.; Torchilin, V. P. siRNA Delivery: From Basics To Therapeutic Applications. *Front. Biosci.* **2013**, *18*, 58–79.
8. Burnett, J. C.; Rossi, J. J. RNA-Based Therapeutics: Current Progress And Future Prospects. *Chem. Biol.* **2012**, *19*, 60–71.
9. Gindy, M. E.; Leone, A. M.; Cunningham, J. J. Challenges In The Pharmaceutical Development Of Lipid-Based Short Interfering Ribonucleic Acid Therapeutics. Expert Opin. *Drug Delivery* **2012**, *9*, 171–182.
10. Dehsorkhi, A.; Castelletto, V.; Hamley, I. W. Self-Assembling Amphiphilic Peptides. *J. Pept. Sci.* **2014**, *20*, 453–467.
11. Hartgerink, J. D.; Beniash, E.; Stupp, S. I. Self-Assembly And Mineralization Of Peptide-Amphiphile Nanofibers. *Science* **2001**, *294*, 1684–1688.
12. Cui, H.; Webber, M. J.; Stupp, S. I. Self-Assembly Of Peptide Amphiphiles: From Molecules To Nanostructures To Biomaterials. *Biopolymers* **2010**, *94*, 1–18.
13. Pashuck, E. T.; Stevens, M. M. Designing Regenerative Biomaterial Therapies For The Clinic. *Sci. Transl. Med.* **2012**, *4*, 160sr164.
14. Hartgerink, J. D.; Beniash, E.; Stupp, S. I. Peptide-Amphiphile Nanofibers: A Versatile Scaffold For The Preparation Of Self-Assembling Materials. *Proc. Natl. Acad. Sci. U.S.A.* **2002**, *99*, 5133–5138.
15. Tysseling-Mattiace, V. M.; Sahni, V.; Niece, K. L.; Birch, D.; Czeisler, C.; Fehlings, M. G.; Stupp, S. I.; Kessler, J. A. Self-Assembling Nanofibers Inhibit Glial Scar Formation And Promote Axon Elongation After Spinal Cord Injury. *J. Neurosci.* **2008**, *28*, 3814–3823.
16. Silva, G. A.; Czeisler, C.; Niece, K. L.; Beniash, E.; Harrington, D. A.; Kessler, J. A.; Stupp, S. I. Selective Differentiation Of

Neural Progenitor Cells by High-Epitope Density Nanofibers. *Science* **2004**, *303*, 1352–1355.
17. Ellis-Behnke, R. G.; Liang, Y. X.; You, S. W.; Tay, D. K.; Zhang, S.; So, K. F.; Schneider, G. E. Nano Neuro Knitting: Peptide Nanofiber Scaffold For Brain Repair And Axon Regeneration With Functional Return Of Vision. *Proc. Natl. Acad. Sci. U.S.A.* **2006**, *103*, 5054–5059.
18. Sang, L. Y.; Liang, Y. X.; Li, Y.; Wong, W. M.; Tay, D. K.; So, K. F.; Ellis-Behnke, R. G.; Wu, W. T.; Cheung, R. T. A Self-Assembling Nanomaterial Reduces Acute Brain Injury And Enhances Functional Recovery In A Rat Model Of Intracerebral Hemorrhage. *Nanomedicine:NBM* **2014**, 10.1016/j.nano.2014.05.012.
19. Palmgren, B.; Jiao, Y.; Novozhilova, E.; Stupp, S. I.; Olivius, P. Survival, Migration And Differentiation Of Mouse tau-gfp Embryonic Stem Cells Transplanted Into The Rat Auditory Nerve. *Exp. Neurol.* **2012**, *235*, 599–609.
20. Mazza, M.; Notman, R.; Anwar, J.; Rodger, A.; Hicks, M.; Parkinson, G.; McCarthy, D.; Daviter, T.; Moger, J.; Garrett, N.; *et al.* Nanofiber-Based Delivery Of Therapeutic Peptides To The Brain. *ACS Nano* **2013**, *7*, 1016–1026.
21. Wagh, A.; Singh, J.; Qian, S.; Law, B. A Short Circulating Peptide Nanofiber As A Carrier For Tumoral Delivery. *Nanomedicine:NBM* **2013**, *9*, 449–457.
22. Mazza, M.; Patel, A.; Pons, R.; Bussy, C.; Kostarelos, K. Peptide nanofibers as molecular transporters: From self-assembly to in vivo degradation. *Faraday Discuss.* **2013**, *166*, 181–194.
23. Bulut, S.; Erkal, T. S.; Toksoz, S.; Tekinay, A. B.; Tekinay, T.; Guler, M. O. Slow Release And Delivery Of Antisense Oligonucleotide Drug By Self-Assembled Peptide Amphiphile Nanofibers. *Biomacromolecules* **2011**, *12*, 3007–3014.
24. Levy, O. A.; Malagelada, C.; Greene, L. A. Cell Death Pathways In Parkinson's Disease: Proximal Triggers, Distal Effectors, And Final Steps. *Apoptosis* **2009**, *14*, 478–500.
25. Laakkonen, P.; Vuorinen, K. Homing Peptides As Targeted Delivery Vehicles. *Integr. Biol.* **2010**, *2*, 326–337.
26. Kostarelos, K.; Lacerda, L.; Pastorin, G.; Wu, W.; Wieckowski, S.; Luangsivilay, J.; Godefroy, S.; Pantarotto, D.; Briand, J. P.; Muller, S.; *et al.* Cellular Uptake Of Functionalized Carbon Nanotubes Is Independent Of Functional Group And Cell Type. *Nat. Nanotechnol.* **2007**, *2*, 108–113.
27. Shalek, A. K.; Robinson, J. T.; Karp, E. S.; Lee, J. S.; Ahn, D. R.; Yoon, M. H.; Sutton, A.; Jorgolli, M.; Gertner, R. S.; Gujral, T. S.; *et al. Proc. Natl. Acad. Sci. U.S.A.* **2010**, *107*, 1870–1875.
28. Robertson, J. D.; Yealland, G.; Avila-Olias, M.; Chierico, L.; Bandmann, O.; Renshaw, S. A.; Battaglia, G. pH-Sensitive Tubular Polymersomes: Formation And Applications In Cellular Delivery. *ACS Nano* **2014**, *8*, 4650–4661.
29. Gilleron, J.; Querbes, W.; Zeigerer, A.; Borodovsky, A.; Marsico, G.; Schubert, U.; Manygoats, K.; Seifert, S.; Andree, C.; Stoter, M.; *et al.* Image-Based Analysis Of Lipid Nanoparticle-Mediated siRNA Delivery, Intracellular Trafficking And Endosomal Escape. *Nat. Biotechnol.* **2013**, *31*, 638–646.
30. Lacerda, L.; Russier, J.; Pastorin, G.; Herrero, M. A.; Venturelli, E.; Dumortier, H.; Al-Jamal, K. T.; Prato, M.; Kostarelos, K.; Bianco, A. Translocation Mechanisms Of Chemically Functionalised Carbon Nanotubes Across Plasma Membranes. *Biomaterials* **2012**, *33*, 3334–3343.
31. Al-Jamal, K. T.; Gherardini, L.; Bardi, G.; Nunes, A.; Guo, C.; Bussy, C.; Herrero, M. A.; Bianco, A.; Prato, M.; Kostarelos, K.; *et al.* Functional Motor Recovery From Brain Ischemic Insult By Carbon Nanotube-Mediated siRNA Silencing. *Proc. Natl. Acad. Sci. U.S.A.* **2011**, *108*, 10952–10957.
32. Beniash, E.; Hartgerink, J. D.; Storrie, H.; Stendahl, J. C.; Stupp, S. I. Self-Assembling Peptide Amphiphile Nanofiber Matrices For Cell Entrapment. *Acta Biomater.* **2005**, *1*, 387–397.
33. Standley, S. M.; Toft, D. J.; Cheng, H.; Soukasene, S.; Chen, J.; Raja, S. M.; Band, V.; Band, H.; Cryns, V. L.; Stupp, S. I. Induction Of Cancer Cell Death By Self-Assembling Nanostructures Incorporating a Cytotoxic Peptide. *Cancer Res.* **2010**, *70*, 3020–3026.
34. Agrawal, A.; Min, D. H.; Singh, N.; Zhu, H. H.; Birjiniuk, A.; von Maltzahn, G.; Harris, T. J.; Xing, D. Y.; Woolfenden, S. D.; Sharp, P. A.; *et al.* Functional Delivery Of siRNA In Mice Using Dendriworms. *ACS Nano* **2009**, *3*, 2495–2504.
35. Yang, J.; Liu, X.; Bhalla, K.; Kim, C. N.; Ibrado, A. M.; Cai, J.; Peng, T. I.; Jones, D. P.; Wang, X. Prevention Of Apoptosis By Bcl-2: Release Of Cytochrome C From Mitochondria Blocked. *Science* **1997**, *275*, 1129–1132.
36. Kuwana, T.; Newmeyer, D. D. Bcl-2-family Proteins And The Role Of Mitochondria In Apoptosis. *Curr. Opin. Cell. Biol.* **2003**, *15*, 691–699.
37. Porter, A. G.; Janicke, R. U. Emerging Roles Of Caspase-3 In Apoptosis. *Cell Death Differ.* **1999**, *6*, 99–104.
38. Li, Y.; Chopp, M.; Jiang, N.; Zhang, Z. G.; Zaloga, C. Induction Of DNA Fragmentation after 10 to 120 minutes of Focal Cerebral Ischemia In Rats. *Stroke* **1995**, *26*, 1252–1257; discussion 1257−1258.
39. Lee, S. H.; Castagner, B.; Leroux, J.-C.; Is There, A. Future For Cell-Penetrating Peptides In Oligonucleotide Delivery? *Eur. J. Pharm. Biopharm.* **2013**, *85*, 5–11.
40. Sakurai, Y.; Hatakeyama, H.; Sato, Y.; Akita, H.; Takayama, K.; Kobayashi, S.; Futaki, S.; Harashima, H. Endosomal Escape And The Knockdown Efficiency Of Liposomal-siRNA By The Fusogenic Peptide SHGALA. *Biomaterials* **2011**, *32*, 5733–5742.
41. Lundberg, P.; El-Andaloussi, S.; Sutlu, T.; Johansson, H.; Langel, U. Delivery Of Short Interfering RNA Using Endosomolytic Cell-Penetrating Peptides. *FASEB J.* **2007**, *21*, 2664–2671.
42. Rahbek, U. L.; Howard, K. A.; Oupicky, D.; Manickam, D. S.; Dong, M. D.; Nielseni, A. F.; Hansen, T. B.; Besenbacher, F.; Kjems, J. Intracellular siRNA And Precursor miRNA Trafficking Using Bioresponsive Copolypeptides. *J. Gene Med.* **2008**, *10*, 81–93.
43. Youn, P.; Chen, Y. Z.; Furgeson, D. Y.; Myristoylated Cell-Penetrating, A. Peptide Bearing A Transferrin Receptor-Targeting Sequence For Neuro-Targeted siRNA Delivery. *Mol. Pharmaceutics* **2014**, *11*, 486–495.
44. Eguchi, A.; Meade, B. R.; Chang, Y. C.; Fredrickson, C. T.; Willert, K.; Puri, N.; Dowdy, S. F. Efficient siRNA Delivery Into Primary Cells By A Peptide Transduction Domain-dsrna Binding Domain Fusion Protein. *Nat. Biotechnol.* **2009**, *27*, 567–U110.
45. Garcia, I.; Martinou, I.; Tsujimoto, Y.; Martinou, J. C. Prevention Of Programmed Cell Death Of Sympathetic Neurons By The Bcl-2 Proto-Oncogene. *Science* **1992**, *258*, 302–304.
46. Chen, J.; Simon, R. P.; Nagayama, T.; Zhu, R.; Loeffert, J. E.; Watkins, S. C.; Graham, S. H. Suppression Of Endogenous Bcl-2 Expression By Antisense Treatment Exacerbates Ischemic Neuronal Death. *J. Cereb. Blood Flow Metab.* **2000**, *20*, 1033–1039.
47. Obeso, J. A.; Rodriguez-Oroz, M. C.; Benitez-Temino, B.; Blesa, F. J.; Guridi, J.; Marin, C.; Rodriguez, M. Functional Organization Of The Basal Ganglia: Therapeutic Implications For Parkinson's Disease. *Mov. Disord.* **2008**, *23* (Suppl 3), S548–559.
48. Limousin, P.; Pollak, P.; Benazzouz, A.; Hoffmann, D.; Le Bas, J. F.; Broussolle, E.; Perret, J. E.; Benabid, A. L. Effect Of Parkinsonian Signs And Symptoms Of Bilateral Subthalamic Nucleus Stimulation. *Lancet* **1995**, *345*, 91–95.
49. Alexander, G. E.; Crutcher, M. D. Functional Architecture Of Basal Ganglia Circuits: Neural Substrates Of Parallel Processing. *Trends. Neurosci.* **1990**, *13*, 266–271.
50. Benabid, A. L.; Chabardes, S.; Mitrofanis, J.; Pollak, P. Deep Brain Stimulation Of The Subthalamic Nucleus For The Treatment Of Parkinson's Disease. *Lancet Neurol.* **2009**, *8*, 67–81.
51. Paxinos, G., Watson, C., Ed. *The Rat Brain In Stereotaxic Coordinate*, Compact 3rd ed.; Academic Press: New York, 1996.
52. McCormack, A. L.; Mak, S. K.; Henderson, J. M.; Bumcrot, D.; Farrer, M. J.; Di Monte, D. A. Alpha-Synuclein Suppression By Targeted Small Interfering RNA In The Primate Substantia Nigra. *PLoS One* **2010**, *5* (e12122), 1–8.

53. Ojala, D. S.; Amara, D. P.; Schaffer, D. V. Adeno-Associated Virus Vectors And Neurological Gene Therapy. *Neuroscientist* **2015**, *21*, 84–98.
54. Marks, W. J., Jr.; Bartus, R. T.; Siffert, J.; Davis, C. S.; Lozano, A.; Boulis, N.; Vitek, J.; Stacy, M.; Turner, D.; Verhagen, L.; *et al.* Gene Delivery Of AAV2-Neurturin For Parkinson's Disease: A Double-Blind, Randomised, Controlled Trial. *Lancet Neurol.* **2010**, *9*, 1164–1172.